

Title

Firstname Lastname¹ , Firstname Lastname² and Firstname Lastname^{2,*}

¹ Affiliation 1; e-mail@e-mail.com

² Affiliation 2; e-mail@e-mail.com

* Correspondence: e-mail@e-mail.com; Tel.: (optional; include country code; if there are multiple corresponding authors, add author initials) +xxx-xxxx-xxx-xxxx (F.L.)

Abstract

Hybrid satellite aerial terrestrial networks (HSATNs) are a promising solution towards tackling coverage and mobility issues in sixth generation (6G) networks. This paper presents a novel transmission scheme in the context of HSATNs, which allows pairs of terrestrial users to be simultaneously served via the satellite and the aerial base station (ABS). To this aim, non-orthogonal multiple access (NOMA) technique is adopted, at the ABS, by applying a rule-based hybrid NOMA and orthogonal multiple access (OMA) schemes. Comparisons between a standalone NOMA-based satellite transmission and the proposed method, reveal that significant sum-rate gains can be harvested under varying system parameters.

Keywords: keyword 1; keyword 2; keyword 3 (List three to ten pertinent keywords specific to the article; yet reasonably common within the subject discipline.)

1. Introduction

The sixth generation (6G) network has already been commenced as a new research initiative, following on from the evolving 5G network. This new type of network envisions sophisticated device-to-device (D2D) and machine-to-machine (M2M) communications, innovative artificial intelligence (AI) techniques, Internet of Everything (IoE) applications connecting people, data, things through processes. Interoperability and convergence between terrestrial and satellite infrastructures will be a prerequisite in the 6G networking. Also, the new space era of non-terrestrial networks (NTNs) comprising of aerial networks, low Earth orbit (LEO) and especially very low Earth orbit (VLEO) satellites has emerged, enabling the path to 6G evolution.

Hybrid satellite-terrestrial networks (HSTNs) have been proposed as an efficient approach towards improving spectral efficiency and increasing the users' reliability all over the world. The available spectrum resources of these networks can be further exploited by adopting the non-orthogonal multiple access (NOMA) principle. However, in the absence of line-of-sight (LoS) conditions, the performance of satellite communication systems is severely deteriorating.

In the context of HSTNs, the unmanned aerial vehicle (UAV)-based communications are expected to improve the performance in various ways. In general, the UAV-aided NOMA schemes have gained the interest of the academia and the industry for various applications in the beyond 5G networks. Focusing on the scenario where the UAVs are adopted in satellite terrestrial communication networks, they could be employed in the NOMA scheme as an intermediate node for increasing the possibility of obtaining LoS conditions.

Received:

Revised:

Accepted:

Published:

Citation: Lastname, F.; Lastname, F.; Lastname, F. Title. *Journal Not Specified* 2025, 1, 0. <https://doi.org/>

Copyright: © 2025 by the authors.

Submitted to *Journal Not Specified* for possible open access publication under the terms and conditions of the Creative Commons Attribution (CC BY) license (<https://creativecommons.org/licenses/by/4.0/>).

All-in-all, and to the best of our knowledge, no studies can be found related to the intelligent integration of aerial and satellite segments in 6G networks by utilizing a hybrid NOMA and orthogonal multiple access (OMA) transmission schemes. Motivated by this observation, in this paper, we propose a novel satellite aerial terrestrial cooperative network scheme, which will be termed SATCON. More specifically, SATCON is formed with the integration of aerial base station (ABS) in the existing satellite network by efficiently combining two unsupervised machine learning (ML) algorithms, namely k-means and k-medoids. Furthermore, the proposed system promotes efficient cooperation between ABS and satellite through an innovative hybrid NOMA/OMA approach, avoiding the waste of resources and energy. Compared to standalone satellite NOMA transmission with optimal user pairing, namely SAT-NOMA, SATCON increases the sum rate and, at the same time, provides higher spectral efficiency for varying satellite channel conditions and ABS bandwidth.

2. Materials and Methods

2.1. UAV-Assisted Downlink Transmission

As shown in Figure 1, the considered SAGIN consists of \mathbf{U} UAVs denoted by $\mathcal{U} = 1, 2, \dots, U$ and \mathbf{S} LEO satellites indicated by $\mathcal{S} = 1, 2, \dots, S$. In addition, \mathbf{K} IoT devices randomly scattered on the ground are represented as $\mathcal{K} = 1, 2, \dots, K$.

In the considered downlink architecture, Internet-of-Things (IoT) devices may either receive data directly from a low Earth orbit (LEO) satellite or be served via an unmanned aerial vehicle (UAV) acting as a decode-and-forward relay. In the latter case, the UAV receives and decodes the satellite downlink signals over the satellite-to-air (S2A) link and forwards the decoded information to ground devices through the air-to-ground (A2G) link.

Within this framework, the satellite performs non-orthogonal multiple access (NOMA) user pairing based on the satellite–user channel conditions and transmits power-domain superimposed downlink signals to each paired user group. Since the unmanned aerial vehicle (UAV) is located within the satellite coverage area, it can also receive and decode the same superimposed signals via the satellite-to-air (S2A) link. In this context, whether the UAV can effectively enhance the downlink performance depends on the transmission capability of its forwarding link. Therefore, the potential benefit of UAV-assisted transmission is determined by the quality of the air-to-ground (A2G) links between the UAV and the ground users.

Accordingly, the UAV evaluates whether auxiliary relaying should be activated and selects the appropriate transmission mode, i.e., NOMA or orthogonal multiple access (OMA), based on the A2G channel conditions. UAV-assisted transmission is enabled only when the achievable downlink rate via the UAV exceeds that of the direct satellite link. Specifically, if a considered user pair can achieve higher downlink rates under the UAV-side NOMA pairing policy, the UAV adopts NOMA transmission to serve this pair. Otherwise, if only a single user benefits from UAV relaying, the UAV selectively serves this user using OMA transmission, while the remaining users continue to be served directly by the satellite.

2.2. Normalized Channel Quality Indicator

2.3. Constraints and Bottlenecks

To characterize the downlink transmission options described above, the satellite downlink is modeled using a land mobile satellite(LMS) channel. The overall channel coefficient between LEO satellite s and UE i is expressed as

$$h_i^s = \sqrt{L_i^s \cdot g_i^s}, \quad (1)$$

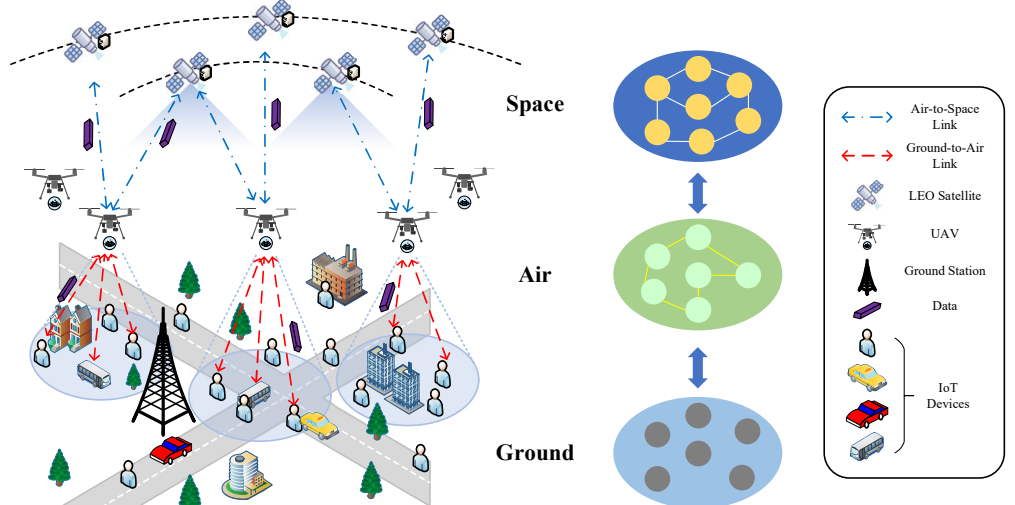


Figure 1. Illustration of the uplink communication procedure in SAGIN, where UAVs act as aerial aggregators to collect data from spatially distributed IoT devices and subsequently offload the aggregated data to LEO satellites.

where L_i^s represents the large-scale free-space path loss given by

$$L_i^s = \left(\frac{c}{4\pi f_c d_i^s} \right)^2, \quad (2)$$

with f_c denoting the carrier frequency, d_i^s the satellite-to-UE distance, and c the speed of light.

The small-scale fading coefficient g_i^s follows the Loo model, characterizing the composite fading as a superposition of a dominant line-of-sight (LoS) component and multipath fading

$$g_i^s(t) = A_i(t)e^{j\phi_i(t)} + m_i(t), \quad (3)$$

where $A_i(t)$ represents the LoS amplitude with $20 \log_{10} A_i(t) \sim \mathcal{N}(\mu, \sigma^2)$, and $m_i(t) = m_{I,i}(t) + j m_{Q,i}(t)$ denotes the multipath component with $m_{I,i}, m_{Q,i} \sim \mathcal{N}(0, \sigma_m^2)$. The parameters are set as $\mu = -1$ dB, $\sigma = 2$ dB, corresponding to a suburban environment.

Furthermore, the Doppler effect induced by satellite motion is captured using the classical Jakes spectrum with maximum Doppler shift $f_D = v f_c / c$, where v denotes the relative velocity between the satellite and UE.

For UAV-assisted transmission, data are forwarded to UEs through an air-to-ground (A2G) link. The channel coefficient between the UAV and UE i is denoted by h_i^d and can be expressed as

$$h_i^d = \sqrt{L_i^{\text{A2G}}} \cdot g_i^d, \quad (4)$$

where L_i^{A2G} represents the large-scale path loss and g_i^d denotes the small-scale fading.

Following the elevation-angle-dependent model by Al-Hourani *et al.* [8], the path loss accounts for probabilistic LoS and NLoS propagation in urban environments. The LoS probability is given by

$$P_{\text{LoS}}(\theta_i) = \frac{1}{1 + a \exp(-b[\theta_i - a])}, \quad (5)$$

where $\theta_i = \arcsin(H/\sqrt{H^2 + d_i^2})$ is the elevation angle, H is the UAV altitude, d_i is the horizontal distance, and (a, b) are environment-dependent parameters. For urban environments, we adopt $a = 9.61$ and $b = 0.16$ [8].

The composite path loss is then computed as

$$L_i^{\text{A2G}} = P_{\text{LoS}}(\theta_i) \cdot L_i^{\text{LoS}} + [1 - P_{\text{LoS}}(\theta_i)] \cdot L_i^{\text{NLoS}}, \quad (6)$$

where

$$L_i^{\text{LoS}}(\text{dB}) = 20 \log_{10} \left(\frac{4\pi f_c d_i^{\text{3D}}}{c} \right) + \eta_{\text{LoS}}, \quad (7)$$

$$L_i^{\text{NLoS}}(\text{dB}) = 20 \log_{10} \left(\frac{4\pi f_c d_i^{\text{3D}}}{c} \right) + \eta_{\text{NLoS}}, \quad (8)$$

with $d_i^{\text{3D}} = \sqrt{H^2 + d_i^2}$ denoting the 3D distance, and $\eta_{\text{LoS}} = 1 \text{ dB}$, $\eta_{\text{NLoS}} = 20 \text{ dB}$ representing the excessive path loss for LoS and NLoS links, respectively [8].

It should be emphasized that the downlink rate delivered to a UE via UAV-assisted relaying is jointly determined by the A2G access link and the satellite-to-UAV (S2A) backhaul. Since the UAV can only forward the data it receives from the satellite, the capacity of the S2A backhaul may limit the effective downlink rate, preventing UAV-assisted transmission from consistently outperforming direct satellite delivery.

All downlink links are assumed to be impaired by additive white Gaussian noise (AWGN). These channel characteristics explain why UAV-assisted relaying may provide significant rate gains for some users while offering no advantage for others, thereby motivating rate-based downlink transmission mode selection.

2.4. ABS placement process

The ABS placement is performed prior to the hybrid transmission decision, since the A2G channel characteristics—and consequently the achievable UAV-assisted rates—are fundamentally determined by the ABS position. Without an appropriately optimized ABS location, the hybrid NOMA/OMA decision would be restricted to a limited set of feasible transmission options, leading to suboptimal system performance.

To facilitate effective hybrid NOMA/OMA downlink decision-making, the ABS placement is designed as a performance-aware structural optimization step rather than an isolated objective. Specifically, the three-dimensional ABS position $\mathbf{p} = (x_1^p, y_1^p, z_1^p)$ is optimized to enhance the quality of the air-to-ground (A2G) channels, which directly determine the achievable UAV-assisted transmission rates. By improving the overall A2G channel conditions through position optimization, the proposed placement strategy enlarges the set of users for which UAV-assisted transmission can provide rate advantages over direct satellite delivery, thereby enabling more effective hybrid NOMA/OMA transmission decisions in the subsequent stage. It is worth noting that the placement optimization does not determine the transmission mode itself, but rather provides a favorable channel structure upon which the subsequent rate-based hybrid decision operates. Based on the above considerations, the ABS placement is formulated as a preliminary, performance-aware optimization step that aims to enhance the air-to-ground (A2G) channel conditions prior to the hybrid transmission decision. Specifically, the three-dimensional ABS position $\mathbf{p} \in W$ is determined by maximizing the aggregate A2G downlink rate experienced by terrestrial users, which is expressed as

$$\arg \max_{\mathbf{p} \in W} \sum_{i \in \mathcal{K}} R_i^d(\mathbf{p}), \quad (9)$$

where W denotes the feasible spatial region for ABS deployment, and $R_i^d(\mathbf{p})$ represents the achievable A2G downlink rate for IoT_i when the ABS is positioned at \mathbf{p} . Since the subsequent hybrid NOMA/OMA transmission decision involves discrete user pairing and

mode selection, a continuous and differentiable surrogate is adopted during the placement phase. In particular, the OMA transmission rate is used as a proxy for the A2G channel quality, given by

$$R_i^d(\mathbf{p}) = B_d \log_2 \left(1 + P_d \Gamma_i^d(\mathbf{p}) \right), \quad (10)$$

where B_d denotes the allocated A2G bandwidth, P_d is the transmission power of the ABS, and $\Gamma_i^d(\mathbf{p})$ is the channel gain experienced by IoT_i, which explicitly depends on the ABS position \mathbf{p} . By optimizing (9) with respect to \mathbf{p} , the proposed placement strategy improves the overall A2G channel quality, thereby providing a favorable rate landscape for the subsequent hybrid NOMA/OMA downlink decision.

The channel gain $\Gamma_i^d(\mathbf{p})$ is determined by the A2G channel model, and depends explicitly on the ABS position \mathbf{p} through the elevation-angle-dependent path loss and the associated line-of-sight probability. In particular, both the horizontal distance between the ABS and IoT_i and the ABS altitude jointly influence the large-scale attenuation, which in turn affects the achievable A2G downlink rate.

The ABS position is restricted by the physical service area and practical deployment constraints of the considered system. Specifically, the horizontal coordinates of the ABS are confined within the coverage region of radius R_{cov} , while the altitude is limited to a feasible range $[z_{\min}, z_{\max}]$ to ensure reliable communication performance and compliance with regulatory requirements. These constraints can be expressed as

$$\begin{aligned} -R_{\text{cov}} &\leq x_1^p \leq R_{\text{cov}}, \\ -R_{\text{cov}} &\leq y_1^p \leq R_{\text{cov}}, \\ z_{\min} &\leq z_1^p \leq z_{\max}, \end{aligned} \quad (11)$$

where R_{cov} denotes the horizontal coverage radius of the service area, and $[z_{\min}, z_{\max}]$ represents the permissible altitude range for ABS deployment, typically set to [50 m, 500 m].

The ABS placement problem in (9) is solved using the Limited-memory Broyden–Fletcher–Goldfarb–Shanno with Box constraints (L-BFGS-B) algorithm, which is suitable for bound-constrained nonlinear optimization. Starting from an initial position \mathbf{p}_0 defined by the geometric centroid of the user distribution in the horizontal plane with a default altitude of 100 m, the algorithm iteratively updates the ABS location based on gradient information until convergence. The convergence tolerance is set to $\epsilon = 10^{-6}$ on the objective function value, with a maximum iteration limit of 100 to ensure computational efficiency.

During the placement phase, the OMA rate in (10) is adopted as a continuous and differentiable surrogate, since the hybrid NOMA/OMA transmission scheme involves discrete user pairing and successive interference cancellation (SIC) operations that are not suitable for gradient-based optimization. The use of the OMA rate allows the placement optimization to focus on improving the A2G channel conditions without imposing any transmission mode decisions.

The optimized ABS position obtained from this procedure is subsequently used as the deployment configuration for the hybrid NOMA/OMA downlink transmission.

2.5. Satellite NOMA transmission

With the ABS position optimized in the previous subsection, we next describe the direct satellite downlink, which constitutes one of the transmission options in the considered system and serves as the benchmark for evaluating whether UAV-assisted delivery can provide a rate improvement.

For the direct satellite downlink, the link quality of each UE l ($1 \leq l \leq N$) is characterized by an equivalent channel gain

$$\Gamma_l^s = \kappa_s |h_l^s|^2, \quad (12)$$

where h_l^s denotes the small-scale fading coefficient of the land mobile satellite (LMS) channel, and κ_s is a constant that accounts for large-scale propagation effects, including path loss, antenna gains, and noise normalization. The defined Γ_l^s serves as a link-quality indicator for computing the achievable rate over the direct satellite path.

UEs are grouped into weak-strong pairs following standard NOMA principles. For each pair, superposition coding is applied at the satellite with total transmit power P_s , where a conventional NOMA power allocation strategy assigns a larger power fraction to the weak UE. Assuming perfect successive interference cancellation (SIC) at the strong UE, the achievable downlink rates over the direct satellite path can be expressed in a unified form as

$$R^s = \frac{B_s}{K} \log_2 \left(1 + \frac{P_s \Gamma^s}{I^s + 1} \right), \quad (13)$$

where Γ^s denotes the corresponding satellite link-quality indicator, and I^s represents the residual intra-pair interference determined by the adopted NOMA power allocation.

The above satellite NOMA transmission serves as a standard transmission option in the considered system and does not involve any optimization over ABS placement, user pairing, or hybrid transmission decisions.

3. Joint Transmission Decision for System Throughput Maximization

3.1. Transmission Options and Decision Variables

With the achievable rates of the direct satellite downlink characterized in the previous section, we now specify the transmission options available to the system and the corresponding decision variables. The objective is to flexibly exploit either direct satellite delivery or UAV-assisted transmission to maximize the overall system throughput.

We consider a set of $N = 2K$ terrestrial UEs grouped into K NOMA pairs. For each UE pair, the system can select one transmission option from a predefined candidate set, which includes direct satellite transmission and ABS-assisted downlink modes. In particular, the following transmission options are available:

- *Direct satellite transmission*: both UEs in the pair are served directly by the satellite using the satellite NOMA scheme described in Section 2.2.
- *ABS-assisted transmission*: the downlink data are delivered to the UE pair via the aerial base station (ABS), where either NOMA or OMA transmission can be employed depending on the channel conditions.

Each transmission option is associated with a corresponding achievable rate determined by the underlying satellite-to-ground or air-to-ground links. Notably, ABS-assisted transmission is activated only when it yields a higher rate contribution than direct satellite delivery; otherwise, the system falls back to pure satellite transmission. This design enables the ABS to be utilized selectively, avoiding unnecessary relaying when the direct satellite link is already sufficient.

Let \mathcal{M}_k denote the set of feasible transmission options for the k -th UE pair. The transmission decision problem can then be interpreted as selecting one option from \mathcal{M}_k for each UE pair, subject to system-level constraints and the overall throughput maximization objective. Importantly, the decision variables are defined at the UE-pair level, while the resulting system performance is evaluated in terms of the aggregate rate across all UEs.

3.2. System-Level Optimization Objective

Based on the transmission options defined in the previous subsection, the objective of the considered system is to maximize the aggregate downlink throughput across all UEs. Rather than optimizing individual links or UE pairs in isolation, a system-level objective is adopted to capture the coupled impact of transmission mode selection, resource sharing, and ABS utilization.

Let R_u denote the achievable downlink rate of UE u , which depends on the selected transmission option for its associated UE pair. The overall system throughput maximization problem is then formulated as

$$\max \quad \sum_{u=1}^N R_u, \quad (14)$$

where the summation is taken over all UEs served by the system. This objective naturally accounts for both direct satellite transmission and ABS-assisted delivery, as well as the interactions among UEs sharing the same transmission resources.

It is important to emphasize that the ABS placement strategy described in Section 2.1 and the satellite NOMA transmission model in Section 2.2 are not optimized independently. Instead, they jointly contribute to the achievable rates R_u and are evaluated through the unified system-level objective in (14). As a result, the system selectively activates UAV-assisted transmission only when it provides a net throughput gain, while reverting to pure satellite transmission in scenarios where ABS assistance is unnecessary or ineffective.

The adoption of a system-wide sum-rate objective enables coordinated transmission decisions across all UE pairs and forms the foundation for the joint decision formulation and iterative optimization framework presented in the following subsections.

3.3. Joint and Coordinated Decision Formulation

Based on the transmission options defined in Section 3.1 and the system-level objective in Section 3.2, the joint transmission decision problem is formulated to coordinate the selection of transmission modes across all UE pairs. Unlike pair-wise greedy selection, the proposed formulation explicitly accounts for system-wide interactions among UE pairs and enables coordinated utilization of satellite and ABS resources.

Let $\mathcal{K} = \{1, \dots, K\}$ denote the set of UE pairs. For each pair $k \in \mathcal{K}$, we define a finite set of feasible transmission options \mathcal{M}_k . Each option $m \in \mathcal{M}_k$ corresponds to a specific combination of transmission links (direct satellite or ABS-assisted) and access schemes (NOMA or OMA), and yields a known achievable rate for the two UEs in pair k .

We introduce a binary decision variable

$$x_{k,m} = \begin{cases} 1, & \text{if transmission option } m \text{ is selected for UE pair } k, \\ 0, & \text{otherwise.} \end{cases} \quad (15)$$

To ensure that each UE pair adopts exactly one transmission option, the following constraint is imposed:

$$\sum_{m \in \mathcal{M}_k} x_{k,m} = 1, \quad \forall k \in \mathcal{K}. \quad (16)$$

Let $R_{k,m}$ denote the aggregate achievable downlink rate of UE pair k when transmission option m is selected. The joint transmission decision problem can then be formulated as the following integer linear programming (ILP) problem:

$$\begin{aligned} \max_{\{x_{k,m}\}} \quad & \sum_{k \in \mathcal{K}} \sum_{m \in \mathcal{M}_k} x_{k,m} R_{k,m} \\ \text{s.t.} \quad & \sum_{m \in \mathcal{M}_k} x_{k,m} = 1, \quad \forall k \in \mathcal{K}, \\ & x_{k,m} \in \{0, 1\}, \quad \forall k \in \mathcal{K}, m \in \mathcal{M}_k. \end{aligned} \quad (17)$$

The formulation in (17) jointly optimizes the transmission decisions of all UE pairs under a unified system-level objective. Different physical transmission behaviors, including activating ABS-assisted transmission for both UEs, for only one UE, or for neither of them, naturally emerge as feasible solutions of the ILP without explicit case enumeration. This unified formulation avoids heuristic rule-based decision making and enables coordinated selection across UE pairs.

In practice, the achievable rates $R_{k,m}$ depend on the ABS placement, channel realizations, and access schemes, and are updated as these system components evolve. While the ILP formulation provides a structured representation of the joint decision problem, its role in this work is to enable coordinated system-level decision making rather than to claim theoretical optimality. Efficient solution strategies and low-complexity alternatives can be employed depending on the system scale and implementation requirements.

3.4. Iterative Joint Optimization Framework

The joint transmission decision problem formulated in the previous subsection is embedded into an iterative system-level optimization framework, which coordinates ABS placement, achievable rate evaluation, and transmission mode selection. The key idea is to progressively refine system decisions based on the resulting throughput performance, rather than relying on a one-shot optimization.

Specifically, the framework operates in an iterative manner. Given an initial ABS position, the achievable rates of both direct satellite transmission and ABS-assisted transmission are evaluated for all UE pairs. Based on these rates, the joint transmission decision problem in (17) is solved to determine the preferred transmission option for each UE pair. The resulting system throughput serves as a performance indicator that implicitly reflects the effectiveness of the current ABS deployment and transmission configuration.

The feedback from the transmission decision to the ABS placement is intentionally designed to be indirect and lightweight. Instead of exchanging detailed per-link information, only the aggregate system throughput is used to guide the subsequent update of the ABS position. This design significantly reduces signaling overhead and computational complexity, while preserving the ability to adapt the ABS deployment to changing network conditions.

An important feature of the proposed framework is its ability to intelligently activate or deactivate ABS-assisted transmission. When ABS assistance provides a throughput improvement, the framework selectively assigns one or both UEs in a pair to ABS-assisted transmission using either NOMA or OMA. Conversely, when direct satellite transmission already achieves satisfactory performance, the system automatically falls back to satellite-only delivery, thereby avoiding unnecessary ABS utilization and conserving aerial and spectral resources.

The iterative process continues until convergence or a predefined stopping criterion is met. Although theoretical convergence guarantees are not explicitly claimed, extensive simulations demonstrate that the proposed framework converges rapidly and yields stable

performance gains. Overall, this iterative joint optimization framework enables coordinated system-level decision making and provides a practical and flexible solution for integrating UAV-assisted transmission into satellite networks.

3.5. baseline

As described previously, ABS is integrated into the satellite network to improve the QoS of terrestrial users. Towards this end, the ABS should first receive and decode the NOMA superimposed signals of each pair of MTs via the S2A channel. The S2A channel gain can be expressed as

$$\Lambda_{sd} = \frac{G_t^s G_r^{sd}}{L_{sd}^{\text{FS}} N_{sd}}. \quad (18)$$

The maximum achievable decoding rates which succeed by the ABS through the S2A channel for each MT_j^s and MT_i^s in pair are

$$R_j^{sd} = \frac{B_s}{K} \log_2 \left(1 + \beta_j^s P_s \Lambda_{sd} \right), \quad (19)$$

$$R_i^{sd} = \frac{B_s}{K} \log_2 \left(1 + \frac{(1 - \beta_j^s) P_s \Lambda_{sd}}{\beta_j^s P_s \Lambda_{sd} + 1} \right). \quad (20)$$

Note that, the ABS obtains all the pair indices from the VLEO through a dedicated control channel to identify the users comprising each pair and their role, e.g., strong or weak satellite channel users. Also, the ABS acquires the achievable rate R_l^s of each MT_l with the satellite, through the same channel.

Next, the ABS should forward the decoded signals to the MTs through the A2G channel, utilizing the proposed hybrid NOMA/OMA transmission scheme. Consequently, we consider that each MT_l reports the CSI of the corresponding A2G link to the ABS. Therefore, the ABS calculates the channel gain of the A2G link for each M Tl as follows

$$\Gamma_l^d = \frac{G_t^d G_r^d}{L_l^{\text{A2G}}(h, r_l) N_d} |h_l^d|^2. \quad (21)$$

Following the same NOMA user pairing policy as the VLEO, the ABS forms K MT pairs, considering now the channel gains of the A2G links. Therefore, each pair consists of the strong A2G channel user MT_j^d , and the weak A2G channel user MT_i^d , where $\Gamma_j^d \geq \Gamma_i^d$. Subsequently, calculates the optimal power allocation factor β_j^d for the MT_j^d by replacing s with d in expression ???. Also, the achievable rates in NOMA, R_j^d and MT_i^d , are given by the expressions ?? and ??, respectively, by replacing again s with d . The rates that ABS can offer to MT_j^d and MT_i^d , utilizing the NOMA technique, are $R_j^{dn} = \min(R_j^d, R_j^{sd})$ and $R_i^{dn} = \min(R_i^d, R_i^{sd})$, respectively.

Lastly, the ABS has to decide whether it is profitable for each pair of MTs to transmit the superimposed signal or to transmit only the signal of one MT of each pair utilizing the OMA technique. Also, the ABS can avoid forwarding the satellite signals if the ABS transmission is not profitable for both MTs in pair. Therefore, the achievable rate that each MT_l can achieve from the ABS through OMA, is equal to

$$R_l^o = \frac{B_d}{K} \log_2 \left(1 + P_d \Gamma_l^d \right). \quad (22)$$

Each MT_l will experience higher rates if the ABS uses OMA, i.e., $R_l^o \geq R_l^d$, since the same bandwidth as NOMA is allocated for OMA transmission, and whole P_d is allocated to MT_l . However, the maximum achievable OMA rate of MT_l is restricted by the expression

$R_l^{do} = \min(R_l^o, R_l^{sd})$, since the ABS may provide a higher rate to the MT_i , but the rate at which ABS decoded its signal from the VLEO is lower and vice versa. There are four different cases that the ABS considers for each MT pair

- **if $R_i^s < R_i^{dn}$ and $R_j^s < R_j^{dn}$:** In this case, the pair of MTs formed by the ABS profits from the NOMA transmission as both MTs achieve greater rates if served from the ABS instead of the satellite.
- **if $R_i^s < R_i^{dn}$ and $R_j^s \geq R_j^{dn}$:** In this case, only MT_i^d profits from the ABS transmission. Thus, the ABS utilizes OMA and transmits only to MT_i^d or the timeslot allocated to this pair. MT_i^d achieves a rate equal to R_i^{do} .
- **if $R_i^s \geq R_i^{dn}$ and $R_j^s < R_j^{dn}$:** In this case, only MT_j^d profits from the ABS transmission. Therefore, the ABS utilizes OMA and transmits only to MT_j^d for the timeslot allocated to this pair. MT_j^d achieves a rate equal to R_i^{do} .
- Otherwise, the communication for this MT pair is not profitable and ABS does not transmit to these pair of users in order to save resources.

4. Results

This section may be divided by subheadings. It should provide a concise and precise description of the experimental results, their interpretation as well as the experimental conclusions that can be drawn.

4.1. Subsection

4.1.1. Subsubsection

Bulleted lists look like this:

- First bullet;
- Second bullet;
- Third bullet.

Numbered lists can be added as follows:

1. First item;
2. Second item;
3. Third item.

The text continues here.

4.2. Figures, Tables and Schemes

All figures and tables should be cited in the main text as Figure 2, Table 1, etc.



Figure 2. This is a figure. Schemes follow the same formatting.

Table 1. This is a table caption. Tables should be placed in the main text near to the first time they are cited.

Title 1	Title 2	Title 3
Entry 1	Data	Data
Entry 2	Data	Data ¹

¹ Tables may have a footer.

The text continues here (Figure 3 and Table 2).

366

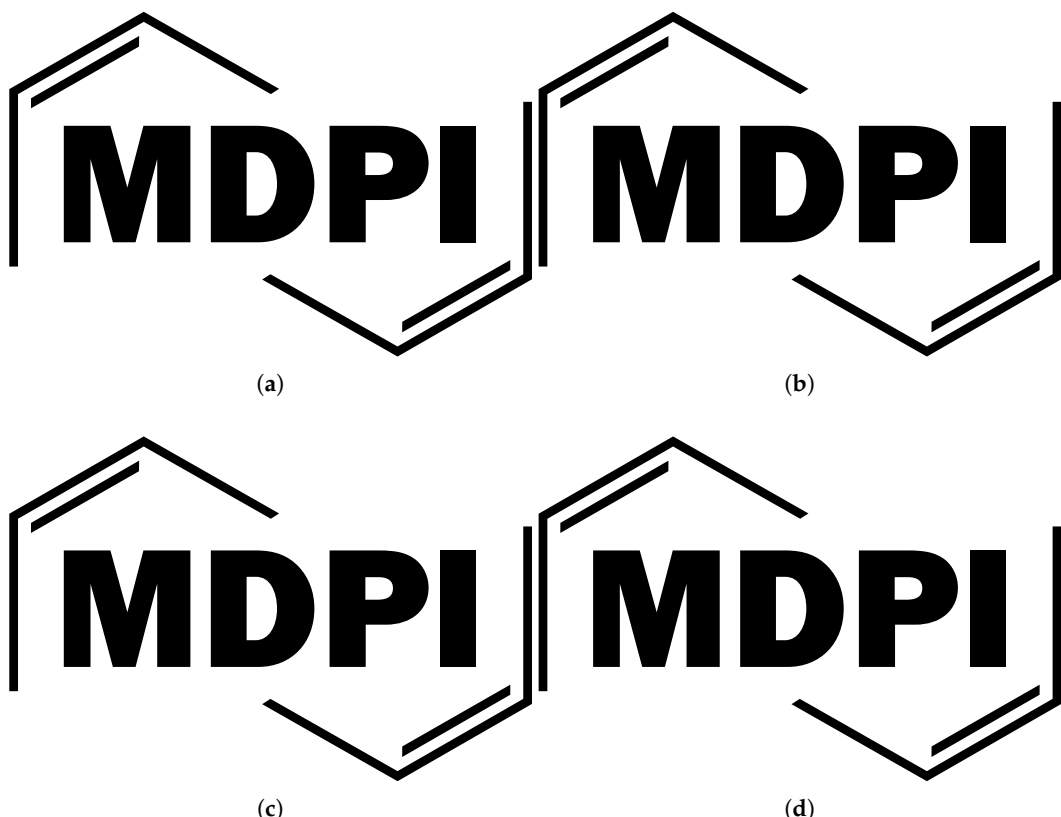


Figure 3. This is a wide figure. Schemes follow the same formatting. If there are multiple panels, they should be listed as: (a) Description of what is contained in the first panel. (b) Description of what is contained in the second panel. (c) Description of what is contained in the third panel. (d) Description of what is contained in the fourth panel. Figures should be placed in the main text near to the first time they are cited. A caption on a single line should be centered.

Table 2. This is a wide table.

Title 1	Title 2	Title 3	Title 4
Entry 1 *	Data Data Data	Data Data Data	Data Data Data
Entry 2	Data Data Data	Data Data Data	Data Data Data

* Tables may have a footer.

367

Text.

368

Text.

369

4.3. Formatting of Mathematical Components

370

This is the example 1 of equation:

371

$$a = 1, \quad (23)$$

the text following an equation need not be a new paragraph. Please punctuate equations as regular text.

372

This is the example 2 of equation:

$$a = b + c + d + e + f + g + h + i + j + k + l + m + n + o + p + q + r + s + t + u + v + w + x + y + z \quad (24)$$

Please punctuate equations as regular text. Theorem-type environments (including propositions, lemmas, corollaries etc.) can be formatted as follows:

Theorem 1. *Example text of a theorem.*

The text continues here. Proofs must be formatted as follows:

Proof of Theorem 1. Text of the proof. Note that the phrase “of Theorem 1” is optional if it is clear which theorem is being referred to. □

The text continues here.

5. Discussion

Authors should discuss the results and how they can be interpreted from the perspective of previous studies and of the working hypotheses. The findings and their implications should be discussed in the broadest context possible. Future research directions may also be highlighted.

6. Conclusions

This section is not mandatory, but can be added to the manuscript if the discussion is unusually long or complex.

7. Patents

This section is not mandatory, but may be added if there are patents resulting from the work reported in this manuscript.

Author Contributions: For research articles with several authors, a short paragraph specifying their individual contributions must be provided. The following statements should be used “Conceptualization, X.X. and Y.Y.; methodology, X.X.; software, X.X.; validation, X.X., Y.Y. and Z.Z.; formal analysis, X.X.; investigation, X.X.; resources, X.X.; data curation, X.X.; writing—original draft preparation, X.X.; writing—review and editing, X.X.; visualization, X.X.; supervision, X.X.; project administration, X.X.; funding acquisition, Y.Y. All authors have read and agreed to the published version of the manuscript.”, please turn to the [CRediT taxonomy](#) for the term explanation. Authorship must be limited to those who have contributed substantially to the work reported.

Funding: Please add: “This research received no external funding” or “This research was funded by NAME OF FUNDER grant number XXX.” and “The APC was funded by XXX”. Check carefully that the details given are accurate and use the standard spelling of funding agency names at <https://search.crossref.org/funding>, any errors may affect your future funding.

Institutional Review Board Statement: In this section, you should add the Institutional Review Board Statement and approval number, if relevant to your study. You might choose to exclude this statement if the study did not require ethical approval. Please note that the Editorial Office might ask you for further information. Please add “The study was conducted in accordance with the Declaration of Helsinki, and approved by the Institutional Review Board (or Ethics Committee) of NAME OF INSTITUTE (protocol code XXX and date of approval).” for studies involving humans. OR “The animal study protocol was approved by the Institutional Review Board (or Ethics Committee) of NAME OF INSTITUTE (protocol code XXX and date of approval).” for studies involving animals. OR “Ethical review and approval were waived for this study due to REASON (please provide a detailed justification).” OR “Not applicable” for studies not involving humans or animals.

Informed Consent Statement: Any research article describing a study involving humans should contain this statement. Please add “Informed consent was obtained from all subjects involved in the study.” OR “Patient consent was waived due to REASON (please provide a detailed justification).” OR “Not applicable” for studies not involving humans. You might also choose to exclude this statement if the study did not involve humans.

Written informed consent for publication must be obtained from participating patients who can be identified (including by the patients themselves). Please state “Written informed consent has been obtained from the patient(s) to publish this paper” if applicable.

Data Availability Statement: We encourage all authors of articles published in MDPI journals to share their research data. In this section, please provide details regarding where data supporting reported results can be found, including links to publicly archived datasets analyzed or generated during the study. Where no new data were created, or where data is unavailable due to privacy or ethical restrictions, a statement is still required. Suggested Data Availability Statements are available in section “MDPI Research Data Policies” at <https://www.mdpi.com/ethics>.

Acknowledgments: In this section you can acknowledge any support given which is not covered by the author contribution or funding sections. This may include administrative and technical support, or donations in kind (e.g., materials used for experiments). Where GenAI has been used for purposes such as generating text, data, or graphics, or for study design, data collection, analysis, or interpretation of data, please add “During the preparation of this manuscript/study, the author(s) used [tool name, version information] for the purposes of [description of use]. The authors have reviewed and edited the output and take full responsibility for the content of this publication.”

Conflicts of Interest: Declare conflicts of interest or state “The authors declare no conflicts of interest.” Authors must identify and declare any personal circumstances or interest that may be perceived as inappropriately influencing the representation or interpretation of reported research results. Any role of the funders in the design of the study; in the collection, analyses or interpretation of data; in the writing of the manuscript; or in the decision to publish the results must be declared in this section. If there is no role, please state “The funders had no role in the design of the study; in the collection, analyses, or interpretation of data; in the writing of the manuscript; or in the decision to publish the results”.

Abbreviations

The following abbreviations are used in this manuscript:

MDPI Multidisciplinary Digital Publishing Institute

DOAJ Directory of open access journals

TLA Three letter acronym

LD Linear dichroism

Appendix A

Appendix A.1

The appendix is an optional section that can contain details and data supplemental to the main text—for example, explanations of experimental details that would disrupt the flow of the main text but nonetheless remain crucial to understanding and reproducing the research shown; figures of replicates for experiments of which representative data are shown in the main text can be added here if brief, or as Supplementary Data. Mathematical proofs of results not central to the paper can be added as an appendix.

Table A1. This is a table caption.

Title 1	Title 2	Title 3
Entry 1	Data	Data
Entry 2	Data	Data

Appendix B

All appendix sections must be cited in the main text. In the appendices, Figures, Tables, etc. should be labeled, starting with "A"—e.g., Figure A1, Figure A2, etc.

References

1. Author 1, T. The title of the cited article. *Journal Abbreviation* **2008**, *10*, 142–149. 459
2. Author 2, L. The title of the cited contribution. In *The Book Title*; Editor 1, F., Editor 2, A., Eds.; Publishing House: City, Country, 2007; pp. 32–58. 460
3. Author 1, A.; Author 2, B. *Book Title*, 3rd ed.; Publisher: Publisher Location, Country, 2008; pp. 154–196. 462
4. Author 1, A.B.; Author 2, C. Title of Unpublished Work. *Abbreviated Journal Name* year, phrase indicating stage of publication (*submitted*; *accepted*; *in press*). 463
5. Title of Site. Available online: URL (accessed on Day Month Year). 465
6. Author 1, A.B.; Author 2, C.D.; Author 3, E.F. Title of presentation. In Proceedings of the Name of the Conference, Location of Conference, Country, Date of Conference (Day Month Year); Abstract Number (optional), Pagination (optional). 466
7. Author 1, A.B. Title of Thesis. Level of Thesis, Degree-Granting University, Location of University, Date of Completion. 468
8. Al-Hourani, A.; Kandeepan, S.; Lardner, S. Optimal LAP Altitude for Maximum Coverage. *IEEE Wireless Commun. Lett.* **2014**, *3*, 569–572. 469

Disclaimer/Publisher's Note: The statements, opinions and data contained in all publications are solely those of the individual author(s) and contributor(s) and not of MDPI and/or the editor(s). MDPI and/or the editor(s) disclaim responsibility for any injury to people or property resulting from any ideas, methods, instructions or products referred to in the content. 471

455

456

457

458

459

460

461

462

463

464

465

466

467

468

469

470

471

472

473